International Journal of Biological Macromolecules 260 (2024) 129541

Contents lists available at ScienceDirect

International Journal of Biological Macromolecules

journal homepage: www.elsevier.com/locate/ijbiomac

Global Lrp regulator protein from *Haloferax mediterranei*: Transcriptional analysis and structural characterization

Laura Matarredona [a,1], María-José García-Bonete [b,1], Jorge Guío [c], Mónica Camacho [a], María F. Fillat [c], Julia Esclapez [a,*], María-José Bonete [a,*]

[a] Departamento de Bioquímica y Biología Molecular y Edafología y Química Agrícola, Grupo Biotecnología de Extremófilos, Universidad de Alicante, San Vicente del Raspeig, Alicante, Spain
[b] Department of Medical Biochemistry and Cell Biology, Institute of Biomedicine. University of Gothenburg, Sweden
[c] Departamento de Bioquímica y Biología Molecular y Celular, Institute for Biocomputation and Physics of Complex Systems, Universidad de Zaragoza, Zaragoza, Spain

ARTICLE INFO

Keywords:
Lrp transcription factor
EMSA
Haloarchaea
X-ray crystallography
SAXS
DSF

ABSTRACT

Haloferax mediterranei, an extreme halophilic archaeon thriving in hypersaline environments, has acquired significant attention in biotechnological and biochemical research due to its remarkable ability to flourish in extreme salinity conditions. Transcription factors, essential in regulating diverse cellular processes, have become focal points in understanding its adaptability. This study delves into the role of the Lrp transcription factor, exploring its modulation of *glnA*, *nasABC*, and *lrp* gene promoters *in vivo* through β-galactosidase assays. Remarkably, our findings propose Lrp as the pioneering transcriptional regulator of nitrogen metabolism identified in a haloarchaeon. This study suggests its potential role in activating or repressing assimilatory pathway enzymes (GlnA and NasA). The interaction between Lrp and these promoters is analyzed using Electrophoretic Mobility Shift Assay and Differential Scanning Fluorimetry, highlighting L-glutamine's indispensable role in stabilizing the Lrp-DNA complex. Our research uncovers that halophilic Lrp forms octameric structures in the presence of L-glutamine. The study reveals the three-dimensional structure of the Lrp as a homodimer using X-ray crystallography, confirming this state in solution by Small-Angle X-ray Scattering. These findings illuminate the complex molecular mechanisms driving *Hfx. mediterranei*'s nitrogen metabolism, offering valuable insights about its gene expression regulation and enriching our comprehension of extremophile biology.

1. Introduction

Haloferax mediterranei is a halophilic archaeon isolated from salterns on the Santa Pola coast (Alicante, Spain) [1] which grows optimally at 2.5 M salt and accumulates, like other haloarchaea, very high concentrations of KCl in its cytoplasm [2]. These conditions challenge protein stability and function, requiring molecular adaptation.

Hfx. mediterranei has been used as a model for studying N-cycle in halophilic archaea, making it attractive for bioremediation in salt, nitrate, and nitrite-rich areas [3–6]. Concerning the nitrogen cycle, this halophile performs denitrification under anaerobic conditions [7,8] and nitrate reduction to ammonium under aerobic conditions (assimilatory pathway). Once nitrate is inside the cell, nitrate and nitrite reductases reduce nitrate to nitrite and nitrite to ammonium, respectively [9,10]. Ammonium produced in this reaction goes through the glutamine synthetase-glutamate synthase (GS-GOGAT) pathway [11,12], which is active when the intracellular ammonium concentration is low. Under nitrogen-abundant conditions, ammonium diffuses across the plasma membrane and is assimilated *via* the glutamate dehydrogenase (GDH) [13,14]. The N-cycle is well characterized biochemically and physiologically, knowing all the enzymes involved and under which conditions they are activated [11,15,16]. However, the transcriptional regulation of this pathway in halophilic archaea is not well-studied. Nitrogen regulatory P-II proteins (GlnK1 and GlnK2) in *Hfx. mediterranei* are known to regulate nitrogen compound assimilation [14,17].

The Lrp transcriptional regulator in *Halobacterium salinarum* has been shown to activate the glutamine synthetase (GS; *glnA*) expression [18]. It has been studied the gene environment of all transcriptional regulators belonging to the Lrp/AsnC family in *Hfx. mediterranei* and was found an Lrp that conserves the gene environment with *Hbt. salinarum*

* Corresponding authors.
E-mail addresses: julia.esclapez@ua.es (J. Esclapez), mjbonete@ua.es (M.-J. Bonete).
[1] Laura Matarredona and María-José García-Bonete contributed equally to this study.

https://doi.org/10.1016/j.ijbiomac.2024.129541
Received 24 November 2023; Received in revised form 3 January 2024; Accepted 14 January 2024
Available online 18 January 2024

[19]. Interestingly, this *lrp* gene was also located downstream of the *glnA* gene, so it was selected as a possible transcriptional regulator of the nitrogen assimilatory pathway. The Lrp/AsnC family is one of Archaea's most abundant transcriptional factors [20,21]. These proteins consist of a DNA-binding domain (helix-turn-helix; HTH domain) for the DNA interaction and a ligand-binding domain (Regulation of Amino acid Metabolism; RAM domain) for the effector binding and/or its oligomerization [22,23]. Studies in different Lrp/AsnC proteins showed that they can bind various amino acids, which affect DNA binding, altering and stabilizing their tertiary and quaternary structures [24–30].

The Lrp from *Hfx. mediterranei* (HFX_RS01210) has been extensively studied using different approaches such as western-blotting assays, characterization of the *lrp* promoter region, and identification of TATA box by site-directed mutagenesis, homologous overexpression of the Lrp protein, deletion mutant, and *in vitro* pull-down DNA-protein binding assays [19,31]. All these previous studies have determined its biochemical characteristics and expression under different stress conditions, including heavy metals and hydrogen peroxide. Focusing on nitrogen assimilation, Lrp may play a role in the transcriptional regulation of nitrogen cycle enzymes, such as GS and assimilatory nitrate reductase (NasA) [31,32].

Further studies of this transcriptional factor have been conducted in this work to elucidate its role and implication in nitrogen metabolism. The involvement of Lrp was analyzed in the regulation of the promoters from *glnA, nasABC,* and *lrp in vivo* using β-galactosidase assays. The interaction of the Lrp protein to the promoters of these genes has also been explored through Electrophoretic Mobility Shift Assay (EMSA) and Differential Scanning Fluorimetry (DSF). In this work, we also present the crystal structure of the Lrp protein from *Hfx. mediterranei* solved at 2 Å by X-ray crystallography and confirming its oligomerization state as a homodimer in solution by Small-Angle X-ray Scattering (SAXS).

2. Materials and methods

2.1. Strains and growth conditions

The *Escherichia coli* strain JM110 was used to prepare unmethylated DNA for efficient transformation of *Hfx. mediterranei.* It was grown in Luria-Bertani medium with ampicillin (100 μg/mL) at 37 °C overnight.

Hfx. mediterranei R4, *Hfx. mediterranei* HM26 (R4-Δ*pyrE2*) [4], the Lrp deletion mutant *Hfx. mediterranei* HM-26-Δ*lrp* [31], and the Lrp overexpression strain *Hfx. mediterranei* Lrp-HM26 [19] were grown at 42 °C in a complex medium (Hm-CM) containing 20 % (*w/v*) seawater (20 % SW) and 0.5 % (*w/v*) yeast extract (pH 7.3).

2.2. Lrp protein overexpression and purification

The Lrp protein was obtained by homologous overexpression in *Hfx. mediterranei* HM26 following the methodology outlined by Matarredona et al. [19]. The *lrp* gene was amplified from the genomic DNA of *Hfx. mediterranei* R4 using specific forward and reverse primers, which include *Eco*RI and *Bam*HI restriction sites. Plasmid construction followed the instructions of the In-Fusion HD cloning kit, maintaining the vector's N-terminal His_6 tag. The ligated product was introduced into *E. coli* DH5α and *E. coli* JM110 through standard transformation. Subsequently, *Hfx. mediterranei* HM26 cells were transformed with pTA1992.*lrp* as described in Pedro-Roig et al. [4] and plated on Hm-MM agar. After incubation at 42 °C for 5–7 days, transformants were selected based on the *pyrE*2 and cultured in Hm-MM. The culture reaching the stationary phase was harvested, and cells were resuspended in an ice-cold binding buffer (20 mM Tris-HCl, 1.5 M NaCl, 30 mM imidazole, pH 7.4). Lysis was achieved by sonication, and the supernatant obtained after centrifugation was collected for protein purification.

The overexpressed protein fraction was purified *via* nickel affinity chromatography, employing a prepacked HisTrap HP 5 mL column according to the manufacturer's guidelines. The bound protein was subsequently eluted in an elution buffer (20 mM Tris-HCl, 1.5 M NaCl, 500 mM imidazole, pH 7.4).

2.3. Analytical size exclusion chromatography (SEC)

The elution fraction from the nickel chromatography was loaded into a second chromatographic step, the analytical SEC using HiPrep 16/60 Sephacryl S-200 HR (Cytiva, Cornella de Llobregat, Spain), to determine the molecular mass of the Lrp in the presence and absence of L-glutamine (L-Gln). The column was pre-equilibrated with a 20 mM Tris-HCl buffer (pH 8.0) containing 1.5 M NaCl. Standard proteins, including apoferritin, glucose dehydrogenase, egg albumin, and cytochrome *c*, were used as markers to estimate molecular mass (Fig. S1). The Lrp protein was prepared at 6 mg/mL concentration in a buffer containing 1.5 M NaCl, 20 mM Tris-HCl, and 30 mM imidazole (pH 7.5). L-Gln was added to a final concentration of 5 mM.

2.4. Promoter activity assay

Three different strains, HM26, HM26-Δ*lrp,* and Lrp-HM26, were individually transformed with three other promoter regions constructions (pVA513.*p.lrp* [31], pVA513.*p.glnA* [33] and pVA513.*p.nasABC* [32]) (Table S1). Transformants were selected using agar plates with 0.3 mg/mL of novobiocin, and β-galactosidase activity was measured throughout the growth curve in two different culture media: defined medium (Hm-DM) with 20 mM NH_4Cl and nitrogen starvation (Hm-NS) [19]. Nitrogen starvation was chosen instead of nitrate as a nitrogen-limiting growth condition, as the deletion mutant HM26-Δ*lrp* cannot grow in the presence of nitrate as a unique nitrogen source. The β-galactosidase assay was performed as previously [19]. All the media were inoculated at OD_{600} 0.02 with pre-adapted cells, and the average and standard error were calculated from the results of three independent cultures.

2.5. Electrophoretic mobility shift assay (EMSA)

EMSA experiments were performed with purified Lrp and two gene promoters (p.*lrp/glnA* and p.*nasABC*) (Table S2). These fragments were generated by PCR with genomic DNA from *Hfx. mediterranei* R4 as a template. The primers used for amplification were p.*lrp/glnA*_For (5′-TTGTCTTCCGTCATTTTCCTGAACAT-3′) and p.*lrp/glnA*_Rev (5′-CGCATCCATGGTTTCGTACGTCAT-3′) for the *lrp/glnA* promoter, p.*nasABC*_For (5′-CAT CCC CCC AAG CTT GCC GGG GCA G-3′) and p.*nasABC*_Rev (5′-ACC ACA CCC CAT GGC ACA GCG CAT-3′) for the *nasABC* promoter. Since *glnA* and *lrp* genes are oriented in opposite directions, the 346 bp promoter fragment for the EMSA assay was designed to include both promoter regions, p.*lrp* and p.*glnA*.

Protein-DNA binding complexes were formed by incubating various concentrations of purified Lrp protein (1.5–7 μM) with 50 ng of the respective promoter (p.*lrp* or p.*nasABC*), along with 50 ng of nonspecific competitor DNA fragment (if*pkn*22, used as control) [34], in binding buffer (10 mM Bis-Tris pH 7.5, 40 mM KCl, 5 % glycerol (*w/v*)), 0.05 mg/mL BSA and 2 mM $MgCl_2$ reaching a final volume of 20 μL. The protein-DNA complexes were subjected to a final concentration of 2 M NaCl for stabilization and facilitation of the binding reaction. When required, different ligands (ammonium, nitrate, 2-oxoglutarate, nickel, cobalt, lithium, or L-Gln) were added to the mixture in the incubation, in the polyacrylamide gel, or in the electrophoresis running buffer to observe their impact on protein-DNA binding. The samples were incubated for 30 min at room temperature and separated on 5 % native polyacrylamide gels in Tris/Borate/EDTA (TBE). The running buffer (TBE 0.5 X with 0.5 M NaCl and 5 mM L-Gln) and the polyacrylamide gel also contained 0.5 M NaCl to maintain high-salt conditions throughout the protein-DNA binding experiments and 5 mM L-Gln. Gels were stained with SYBR® Safe (Invitrogen, Carlsbad, CA, USA).

2.6. Differential scanning fluorimetry (DSF)

DSF experiments were performed using 10 μM of Lrp protein and 5× of SYPRO Orange in different conditions using a total reaction volume of 25 μL. The protein was diluted in the different buffers for the buffer screening and salt stability study, and SYPRO Orange was mixed into the reaction. Buffers contain 50 mM of the buffer type (Tris-HCl, MES, Hepes) and 0.25 M or 1.5 M NaCl in low and high salt, respectively. In all the DSF experiments presented, the temperature was ramped up by 0.2 degrees per minute from 25 to 95 °C using the StepOnePlus Applied Biosystems PCR System from ThermoFisher to get the melting curves. The Tm was estimated using generated first derivative plots from the AppliedBiosystems™StepOne™software v2.3. All the experiments, except for the buffers screening, were performed in 50 mM MES pH 6.5, 1 mM $MgCl_2$ (0.25 M or 1.5 M NaCl), and three replicates that were averaged and plotted. The effect of the KCl salt was studied by substituting NaCl but maintaining all the other parameters the same.

L-Gln effect in Lrp stability was analyzed by adding 180 μM L-Gln into the reaction. For diagnosing the effect of the Lrp protein (10 μM) binding to the promoters, two types of dsDNA promoters were used: one of 346 bp including the *lrp* and *glnA* promoter at 20 μM (Table S2) and shorter ones, including 30 bp of *lrp, glnA* and *nasABC* at 30 μM (Table S3). Ten minutes of incubation at room temperature was performed before SYPRO Orange addition to ensure Lrp protein binding to the DNA promoter.

To generate the short dsDNA promoters, primers of 30 bp and their complementary strands for each promoter were purchased from Isogen Life Science. These oligonucleotides (5′-ACTATAAAGACCTTTCCGCTTAATGCAATT-3′(30-mer, p.*lrp*), 5′-GTAATGACGTACGAAAACGTCGATGCGAAG-3′ (30-mer,p.*glnA*), 5′-ATTCTTAGTATACGTTTGTAGATTGCACGA-3′ (30-mer,p.*nasABC*) were annealing with their complementary to form dsDNA by mixing 1:1 ratio (100 μM) of each primer and incubating at room temperature.

2.7. Protein crystallization

Before crystallization, Lrp was purified by size-exclusion chromatography using a Superose® 6 Increase 10/300 GL (Cytiva) in an ÄKTA Explorer FPLC System and 10 mM Tris-HCl pH 8.0 and 1.5 M NaCl buffer. The protein was concentrated using a Vivaspin-20 of 5 kDa cutoff to 10 mg/mL and subjected to crystallization screening using Mosquito LCP robot (TTPLabtech). The crystals were grown in MRC2/3 plates (Molecular Dimensions) using the sitting-drop vapour diffusion method at 20 °C. Drops contained three different ratios: 1:1 (100 nL + 100 nL), 2:1 (200 nL + 100 nL), and 1:2 (100 nL + 200 nL) of protein and reservoir, respectively, were equilibrated against a 50 μL reservoir using the Proplex, PACT premier, LMB, Clear Screening I, Clear Screening II and JCSG+ screening kits from Molecular Dimensions. Thin needle crystals grew after 1–2 weeks from the B7 condition of the Proplex screening (0.1 M sodium acetate pH 4.0, 0.2 M ammonium acetate 15 % *w/v* PEG 4000) and were further optimized. High-resolution diffracting crystal (300–400 μm long; Fig. S2) grew in 0.1 M sodium acetate pH 3.6, 0.2 M ammonium acetate, 10 % PEG 4000, 20 % ethylene glycol, and 4 mg/mL protein. Crystals were already cryo-protected by adding ethylene glycol into the reservoir condition and flash-cooled in liquid nitrogen.

2.8. X-ray data collection, structure determination, and refinement

Diffraction data was collected on the 18th of March 2022 in the Biomax beamtime of MAXIV synchrotron in Lund, Sweden, using a DECTRIS EIGER X 16 M detector. Data collection parameters can be found in Table S4. The data set was processed, integrated, and scaled using XDS-package [35]. The phases were determined by molecular replacement method using the monomer structure of putative HTH-type transcriptional regulator PH119 from *P. horikoshii* OT3 (PDB ID: 2E1C) [36] as a search model in Phaser [37] of the Phenix software suit [38,39]. Phenix AutoBuild [40] was used for the model building. After rebuilding, the model was taken for the successive manual and automatic refinement steps with Coot [41] and Phenix Refine [42]. A summary of data collection and refinement statistics is given in Table S4. The coordinates and structure factors have been deposited to the Protein Data Bank (PDB ID: 8Q90), and the diffraction images have been deposited in Integrated Resource for Reproducibility in Macromolecular Crystallography (IRRMC ID: TBA).

2.9. Small angle X-ray scattering (SAXS)

SAXS measurements were performed at the BM29 beamline of the European Synchrotron Radiation Facility, Grenoble, France, according to the parameters described in Table S5. A Pilatus 1 M detector in vacuum was used to record the q range of 0.03–5 nm^{-1} and $\lambda = 0.099$ nm with 1 s exposure per frame. Scattering data was collected in batch mode from serial dilution samples of Lrp protein (from 2 mg/mL to 0.25 mg/mL). In addition, three buffer conditions were analyzed: 50 mM Tris-HCl pH 8.0 in 0.5 M, 1 M, and 1.5 M NaCl concentration. The batch mode experiments were performed with the automated sample changer of the beamline and filtered samples at 20 °C. Data reduction and 1D scattering intensities of the sample were done at the beamline BM29. Frames selection, averaging, buffer subtraction, and extrapolation were performed using primusqt [43] from the ATSAS 3.0.0 package [44]. The radius of gyration (Rg), forward scattering (I(0)), maximum particle dimension (Dmax), and the distance distribution function were determined with GNOM [45] and described in Table S5 and Fig. S3. The molecular mass was obtained using the Bayesian inference approach [46] with the ATSAS package. Initial *ab initio* models were obtained by running dummy atom modelling DAMMIN [47]. The final model was used to fit the Lrp homodimer structure obtained from X-ray crystallography using UCSF ChimeraX [48,49]. Crysol was used to compare the experimental scattering curve with the calculated one from the crystal structure. The SAXS results are deposited to SASBDB with accession number SASDT82.

3. Results

3.1. In vivo characterization of lrp, glnA, and nasABC promoter regulation by the Lrp transcription factor

Previous studies have shown that Lrp recognizes its promoter and the p.*nasABC* promoter *in vitro* in the presence of ammonium or nitrate as nitrogen sources, thereby regulating gene expression [31,32]. To investigate whether the transcriptional regulator Lrp is linked to the activation of genes in the nitrogen assimilatory pathway, β-galactosidase activity measurements were carried out to characterize the promoters of glutamine synthetase (p.*glnA*), assimilatory nitrate reductase (p.*nasABC*) and its own promoter (p.*lrp*) (Table S1) in three strains: HM26 (control), HM26-Δ*lrp* (deletion mutant strain) and Lrp-HM26 (overexpression strain).

In the presence of ammonium, Lrp demonstrates positive autoregulation. While the HM26-Δ*lrp* strain showed no significant differences compared to the control, the overexpression strain Lrp-HM26 exhibited an increased β-galactosidase activity, indicating a slight positive modulation by Lrp (Fig. 1A). Concerning p.*nasABC*, β-galactosidase activity levels approached zero when ammonium was the nitrogen source [32]. Fig. 1C illustrates that no promoter-specific activity was detected in either the control (HM26) or the overexpression strain (Lrp-HM26). When the regulator is not present (HM26-Δ*lrp*), some promoter activity appears. Despite not reaching 0.1 U/mg, the transcriptional regulator may negatively modulate the p.*nasABC* under ammonium conditions. Similar trends were observed for the GS promoter (p.*glnA*), where the absence of Lrp led to increased activity, reaching values up to 4 U/mg at 60 h, while Lrp overexpression resulted in decreased activity (0.25 U/

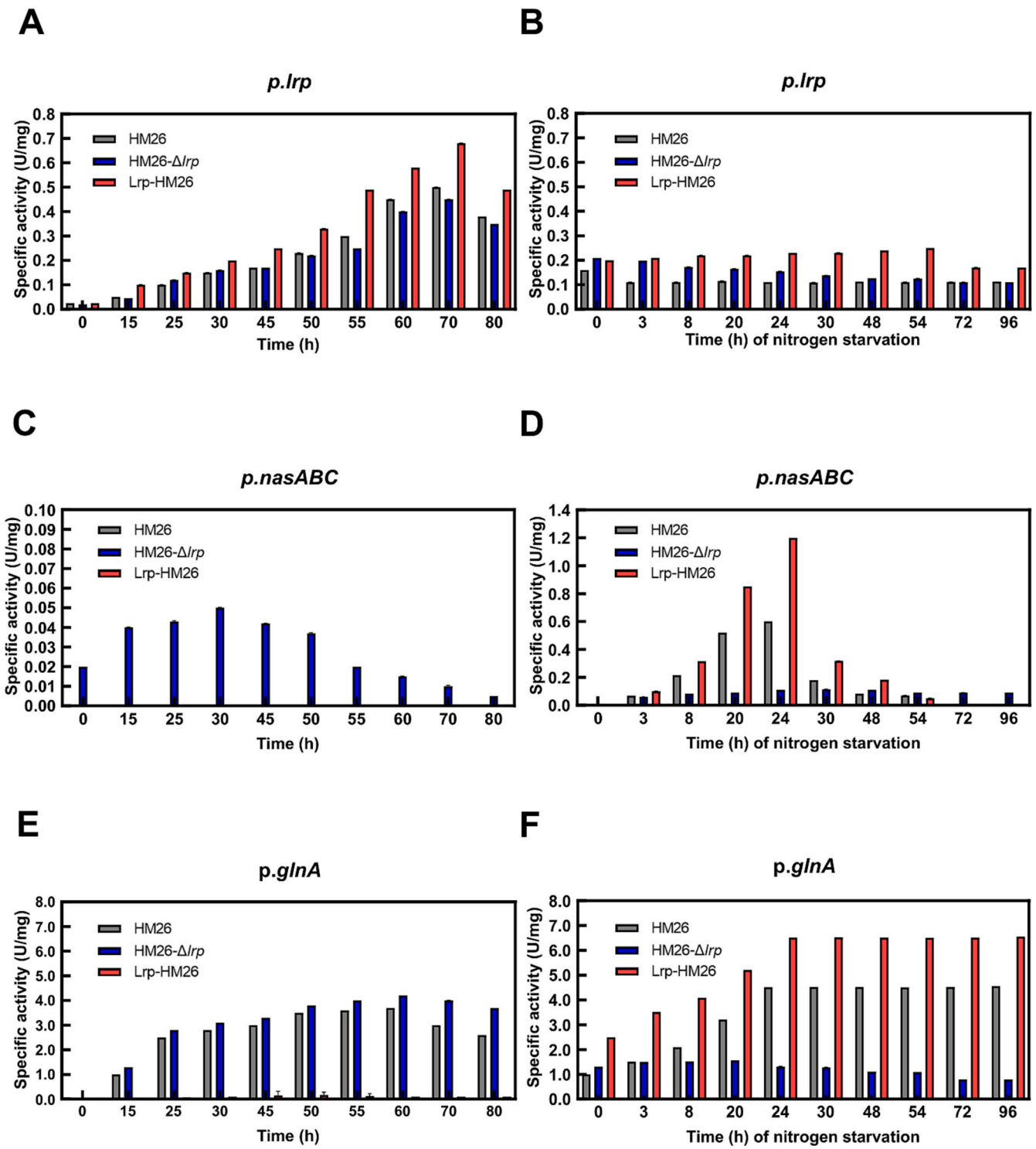

Fig. 1. β-galactosidase specific activity driven by p.*lrp*, p.*glnA*, and p.*nasABC* in extracts from *Hfx. mediterranei* HM26 (control; grey), HM26-Δ*lrp* (deletion mutant; blue), and Lrp-HM26 (overexpression strain; red) growth with 20 mM ammonium (**A, C, E**) as nitrogen source and under nitrogen starvation until 96 h (**B, D, F**).

mg) (Fig. 1E). Based on these results, it can be hypothesized that Lrp also represses this promoter, considering that GS and NasA are less active under nitrogen-rich conditions than in nitrate.

In nitrogen-limited conditions, p.*lrp* exhibited positive autoregulation, with Lrp-HM26 showing higher activity than the control after 24 h (Fig. 1B). Otherwise, gene expression of both GS and NasA was positively regulated by Lrp; the transcriptional regulator activates both promoters under low nitrogen conditions. β-galactosidase activities increased in the Lrp-overexpressing strain (Lrp-HM26). In the characterization of p.*nasABC* during nitrogen starvation, HM26-Δ*lrp* yielded a minimal basal activity of approximately 0.1 U/mg (Fig. 1D). Therefore, NasA expression was not induced if the transcriptional regulator was absent. When Lrp was overexpressed (Lrp-HM26), the β-galactosidase activity driven by p.*nasABC* regained activity but was markedly higher than in HM26, reaching 1.2 U/mg at 24 h. The p.*gln*A exhibited very high activity values of around 4 U/mg of β-galactosidase in the control strain (Fig. 1F). However, in the overexpression strain (Lrp-HM26), β-galactosidase under the control of the p.*glnA* reached

values of 6.5 U/mg from 24 h and maintained its activity over time. Values below half the regular promoter activity were detected without Lrp (HM26-Δ*lrp)*.

3.2. *In vitro interactional studies of the Lrp protein with lrp, glnA, and nasABC promoter regions*

Previous *in vitro* pull-down assays demonstrated Lrp's ability to recognize specific binding sites within the assimilatory NasA promoter (p.*nasABC*) [32] and the *lrp* promoter (p.*lrp*) [31] (Table S2). Electrophoretic Mobility Shift Assays (EMSA) were conducted to elucidate the conditions promoting specific protein-DNA complex formation. Initial attempts focused on the *lrp* promoter region to optimize this technique in halophilic archaea, a field with limited EMSA research [50]. Given the structural preservation requirements of halophilic proteins, the assays were performed with 0.5 M NaCl. To identify a potential effector molecule for the Lrp protein, different possible ligands were used in the EMSA assay with a constant protein concentration of 7 μM, which was optimized previously (Fig. 2A). Ligands were chosen based on the potential function of the transcriptional regulator in nitrogen metabolism (ammonium, nitrate, 2-oxoglutarate, and L-Gln) and in response to metal stress (cobalt, lithium, and nickel). To discard the non-specific binding of Lrp, a competitor DNA consisting of 50 ng of the internal fragment of gene *pkn22* (if*pkn22*) from the cyanobacterium *Anabaena sp.* PCC7120 was used as control. This screening revealed that Lrp has a higher binding affinity to the promoter region in the presence of 5 mM L-Gln. This is the only ligand whose assay resulted in two bands: the Lrp-DNA complex and an unbound portion of the promoter. Other ligands did not affect the DNA-binding properties of Lrp, and no shift was observed. These results confirm that L-Gln enhances the binding specificity of Lrp in the promoter regions of *lrp/glnA* genes. Subsequent EMSAs were performed to explore different L-Gln concentrations (1–3 mM) to enhance band shifts (Fig. 2B). It was obtained complex formation at all tested concentrations of L-Gln; however, part of the promoter does not bind to the protein. As a trial to improve complex formation, a concentration of 2.5 mM L-Gln was added to the gel and electrophoresis buffer, dramatically improving the results (Fig. 2C). Not only was the optimal protein concentration observed to facilitate binding, but full binding of the promoter to the protein was achieved, as a very thick delayed band was obtained. After optimizing the EMSA conditions, the interaction between Lrp and p.*nasABC* was analyzed (Fig. 2D). The conditions are the same as with the previous promoter, as full binding is obtained at 7 μM protein and with L-Gln throughout the EMSA assays.

Differential Scanning Fluorimetry (DSF) was employed to understand further the interaction between the Lrp protein and the dsDNA [51]. This technique allows us to detect the binding of Lrp protein to the promoters' double-stranded DNA by measuring the protein's thermal stability in the presence and absence of L-Gln (Fig. 2 E-H and Fig. S4). By measuring the SYPRO Orange fluorescent during thermal denaturation of the Lrp protein, we can detect a shift in the melting temperature (Tm) of the protein produced by the dsDNA binding. In Fig. 2E and F, the binding of the Lrp protein to the *lrp/glnA* promoter, used in the EMSA studies (Table S2), was analyzed in the absence of L-Gln. To narrow down the DNA binding regions of the *lrp, glnA*, and *nasABC* promoters and to discriminate between the interaction with the *lrp* and the *glnA* promoters, 30 bp dsDNA regions of each promoter were selected (Table S3) and tested for interaction with the halophilic Lrp protein using DSF (Fig. S4). These results suggest that the binding of Lrp protein to the promoter regions in the absence of L-Gln destabilizes the protein (probably from the RAM domains), showing a decrease in the melting temperature when the dsDNA is present. However, in the presence of 180 μM L-Gln (Fig. 2G, H), the Tm shift increases around 0.8–1.5 °C when the Lrp protein is bound to the promoters, suggesting that the binding of L-Gln to the Lrp protein stabilizes the protein: DNA complex as observed in the EMSA assays. The results also show that the higher shift in temperature occurs in the binding of the Lrp protein to the *gln*A promoter (Fig. 2G, H, and Fig. S4), being the best candidate, as we expected.

3.3. *L-glutamine binding studies to the Lrp transcription factor*

L-Gln has been identified as a ligand for certain Lrp/AsnC proteins [52] (ID PDB: 2CYY). Analytical size exclusion chromatography (SEC) (Fig. 3A) revealed that in the presence of L-Gln, the Lrp protein forms an octameric structure with an experimental molecular mass of approximately 128 kDa. Conversely, in the absence of L-Gln, Lrp exists as a dimer with a molecular mass of 32 kDa (Fig. 3A). In addition to the chromatographic studies and EMSA assays, we evaluated the interaction between L-Gln and Lrp by DSF (Fig. 3B, C). The melting temperature increased by approximately 2–4 degrees at low/high NaCl concentrations, indicating that the protein is stabilized in the presence of L-Gln.

3.4. *Structural characterization of the Lrp transcription factor from Hfx. mediterranei*

The Lrp protein structure has been solved at 2 Å by X-ray crystallography, suggesting a homodimer in this crystal condition (Fig. 4). Structural data and analysis are in the supplementary Table S4 and S5.

One molecule of the Lrp protein consists of two domains (Fig. 4A): the HTH domain for DNA binding and the RAM domain for ligand binding and tetramer/octamer oligomerization (Fig. 4A). The HTH domain at the N-terminal is formed by three α-helix (α1-α2-α3) and one β strand (β1) involved in homodimerization, creating an intermolecular antiparallel β-sheet (β1- β1'). The RAM domain at the C-terminal is formed by one antiparallel β-sheet and two α-helix (α4- α5). That antiparallel β-sheet consists of five β-strands, four of them from one molecule (β2- β3- β4- β5) and the last one belonging to a second molecule (β6'). The biological unit of this transcription factor is a homodimer stabilized by three antiparallel intermolecular β-sheets (β1- β1', β2- β3- β4- β5- β6' and β2'- β3'- β4'- β5'- β6) (Fig. 4A).

Although other transcription factors from this family have been crystallized as octamers in other species, a dimeric form was found in the crystal packing for *Hfx. mediterranei* Lrp protein. SAXS confirmed our crystallography results about being a homodimer in solution with a radius of gyration (Rg) 2.42 nm (Fig. S3 A, C). The Pr function also shows a globular shape with a maximum particle dimension (Dmax) of 7.9 nm (Fig. S3 D, E), and the Kratky plot suggests a well-folded globular protein (Fig. S3 B). The comparison of the scattering curve with the calculated from the crystal structure highly agrees with a χ^2 of 1.287, suggesting that this dimeric form is not highly flexible in solution (Fig. 4B), which might be related to the intermolecular β-sheets that keep the molecule stabilized.

Halophilic Lrp from *Hfx. mediterranei* shows a highly acidic surface compared to other mesophilic bacteria and thermophilic archaea, as illustrated in Fig. 4C.

3.5. *Stability studies of the Lrp transcription factor*

DSF was also used to test the Lrp protein's stability using different buffer conditions and to monitor its melting temperature (Tm) shift. The buffers were 50 mM MES, Hepes, and Tris-HCl, covering a range of pH values from 5.5 to 9.0 and two NaCl concentrations (0.25 M and 1.5 M) (Fig. 5A and B).

The results showed that the MES buffer at pH 6.5 maintains the stability of Lrp protein longer when the temperature rises. In addition, the presence of 1.5 M NaCl, like in other halophilic proteins [54–58], plays an essential role in stabilizing this protein, increasing its melting point 18 degrees higher than in low salt (Fig. 5C and D). Moreover, the effect of different concentrations of NaCl was also evaluated using SAXS (Fig. S5). Although the high salt concentration increases the stability of the Lrp protein against temperature, no difference was observed in the scattering profiles at low and high salt (Fig. S5A). Neither partial

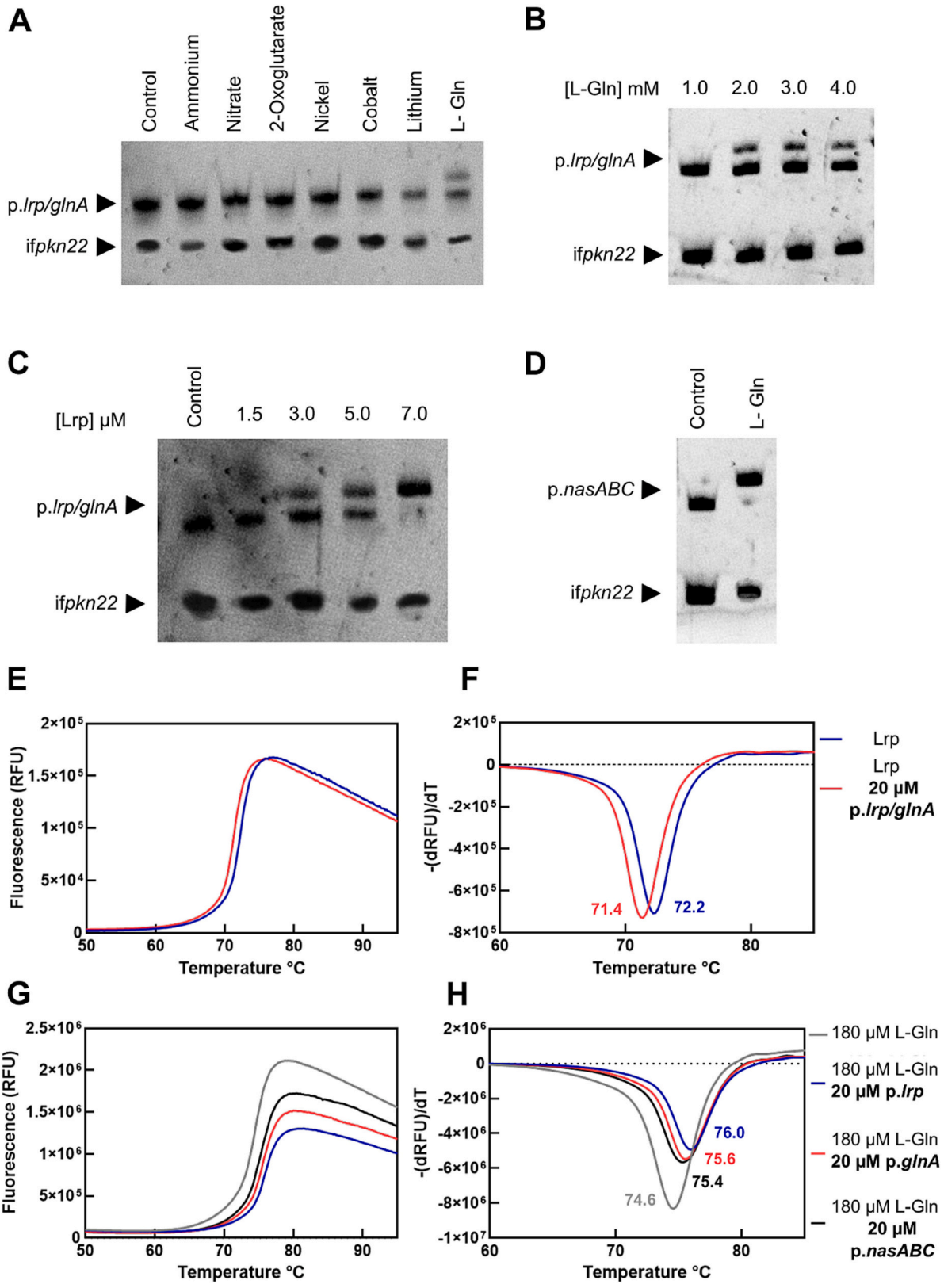

Fig. 2. EMSAs of the Lrp protein binding to the promoter regions of *lrp/glnA* and *nasABC*. **A.** EMSAs using different ligands. **B.** EMSAs using different concentrations of L-Gln. **C.** EMSAs showing the binding of different concentrations of the Lrp protein to the p.*lrp/glnA*. **D.** EMSAs showing the binding of Lrp to p.*nasABC*. **E** and **F.** DSF experiments of Lrp in the presence of the 350 bp dsDNA promoter from *lrp/glnA* in 50 mM MES pH 6.5, 1.5 M NaCl and 1 mM $MgCl_2$. Melting curve (**E**) and first derivative (**F**). **G** and **H.** DSF experiments of Lrp in the presence of the 30 bp dsDNA promoters from *lrp, glnA,* and *nasABC* genes. Melting curve (**G**) and first derivative (**H**).

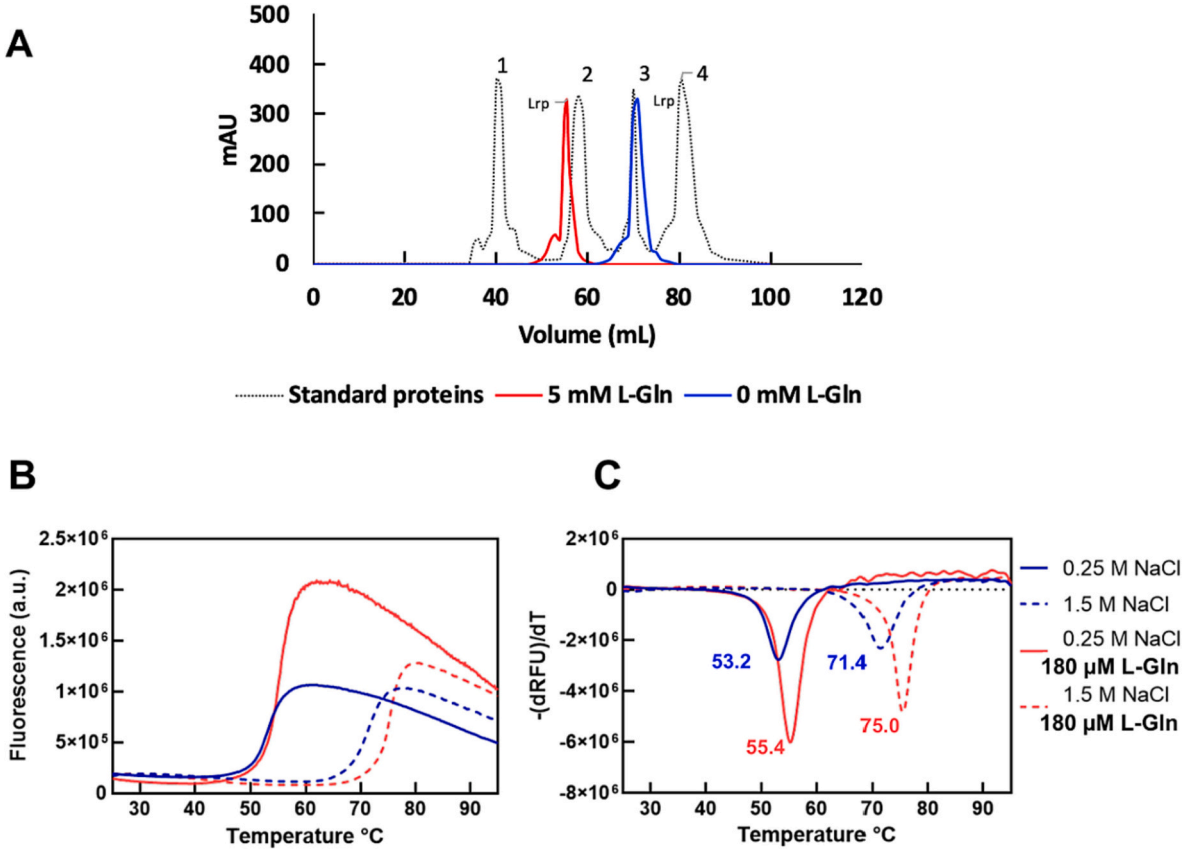

Fig. 3. L-Gln effect in Lrp oligomerization state and stability. **A.** Analytical size exclusion chromatography of Lrp with and without L-Gln (1: apoferritin (443 kDa); 2: glucose dehydrogenase (79 kDa); 3: egg albumin (45 kDa); 4: cytochrome *c* (12.5 kDa)). **B** and **C.** DSF experiments with L-Gln (red) and without (blue), melting curve, and first derivate, respectively.

unfolding of the protein was noticed in their Kratky plots (Fig. S5B).

In Fig. 5 (C, D), we also evaluated the stability effect that KCl has on the Lrp protein compared with NaCl. The results show that this protein's Tm increases when KCl is used. At lower concentrations of salt (0.25 M), the effect of KCl is more pronounced than at high concentrations of salt (1.5 M). These results also agree with previous studies of other halophilic proteins [54–58]; it has been extensively described that KCl is the predominant salt in the haloarchaea cytoplasm.

4. Discussion

This study substantially advances our comprehension of the transcriptional regulator Lrp in *Hfx. mediterranei*, providing insights into its role in nitrogen metabolism and revealing its structural characteristics. The enzymes involved in the nitrogen assimilatory pathway have been biochemically purified and characterized providing valuable insights into their activity under specific physiological conditions. However, there are still numerous unknowns' proteins concerning the regulatory mechanisms governing gene expression in this pathway within *Hfx. mediterranei* and haloarchaea.

The study meticulously characterizes three promoters (p.*nasABC*, p. *lrp*, and p.*glnA*) in three strains of *Hfx. mediterranei*: HM26 (control), HM26-Δ*lrp* (deletion mutant), and Lrp-HM26 (overexpression strain). Using β-galactosidase as a reporter gene, the results confirm that Lrp activates the expression of GS and NasA under nitrogen-limiting conditions while repressing their expression in the presence of ammonium. These findings align with previous observations regarding genes involved in the nitrogen assimilation pathway [5,11,32].

Previous research on *Sulfolobus acidocaldarius* revealed that L-Gln acts as the effector of Sa-Lrp, enhancing DNA-binding affinity and sequence specificity by inducing the formation of octamers [27]. In this work, EMSA and DSF assays highlight the crucial role of L-Gln in stabilizing protein-DNA complexes despite the differences in organisms and protein families (Fig. 2). Gel filtration chromatography reveals the transition of Lrp into an octameric form in the presence of L-Gln, emphasizing the importance of diverse effector molecules observed in different organisms [36,59] for its oligomerization. The formation of a higher oligomerization state of the Lrp protein in presence of L-Gln aligns well with its increased in stability in the DSF experiments. While our findings underscore the value of glutamine in this context, it may not be necessary for other Lrp proteins. For instance, *Hbt. salinarum* utilizes L-aspartate as its effector molecule, while FL11 from the hyperthermophilic archaeon *Pyrococcus* OT3 employs L-lysine for octamer assembly and DNA binding, and FL5 from *Pyrococcus horikoshii* uses L-phenylalanine, L-isoleucine, L-leucine, L-valine, and L-methionine [36,59]. Several observations reinforce the involvement of Lrp in nitrogen metabolism: i) a complete deletion mutant could not be generated due to the essential role of the *glnA* enzyme in *Hfx. mediterranei*; eliminating Lrp would also remove a critical region for *glnA* expression, thus a partial mutant was performed [31]; ii) the partial mutant does not grow in the presence of nitrate as a nitrogen source, suggesting the essential role of this Lrp in nitrate assimilation in this microorganism; iii) for the DNA-protein interaction assay, EMSA, L-Gln was indispensable; iv) pull-down assays using p.*nasABC* and p.*lrp* demonstrated binding to the transcriptional regulator Lrp [31,32].

Furthermore, the structure of Lrp protein from *Hfx. mediterranei* has been solved by X-ray crystallography, being the first transcriptional factor of this type obtained from a halophilic archaeon. While limited information exists about 3D structures of halophilic proteins binding DNA, only one example corresponds to RosR from *Hbt. salinarum*, with a

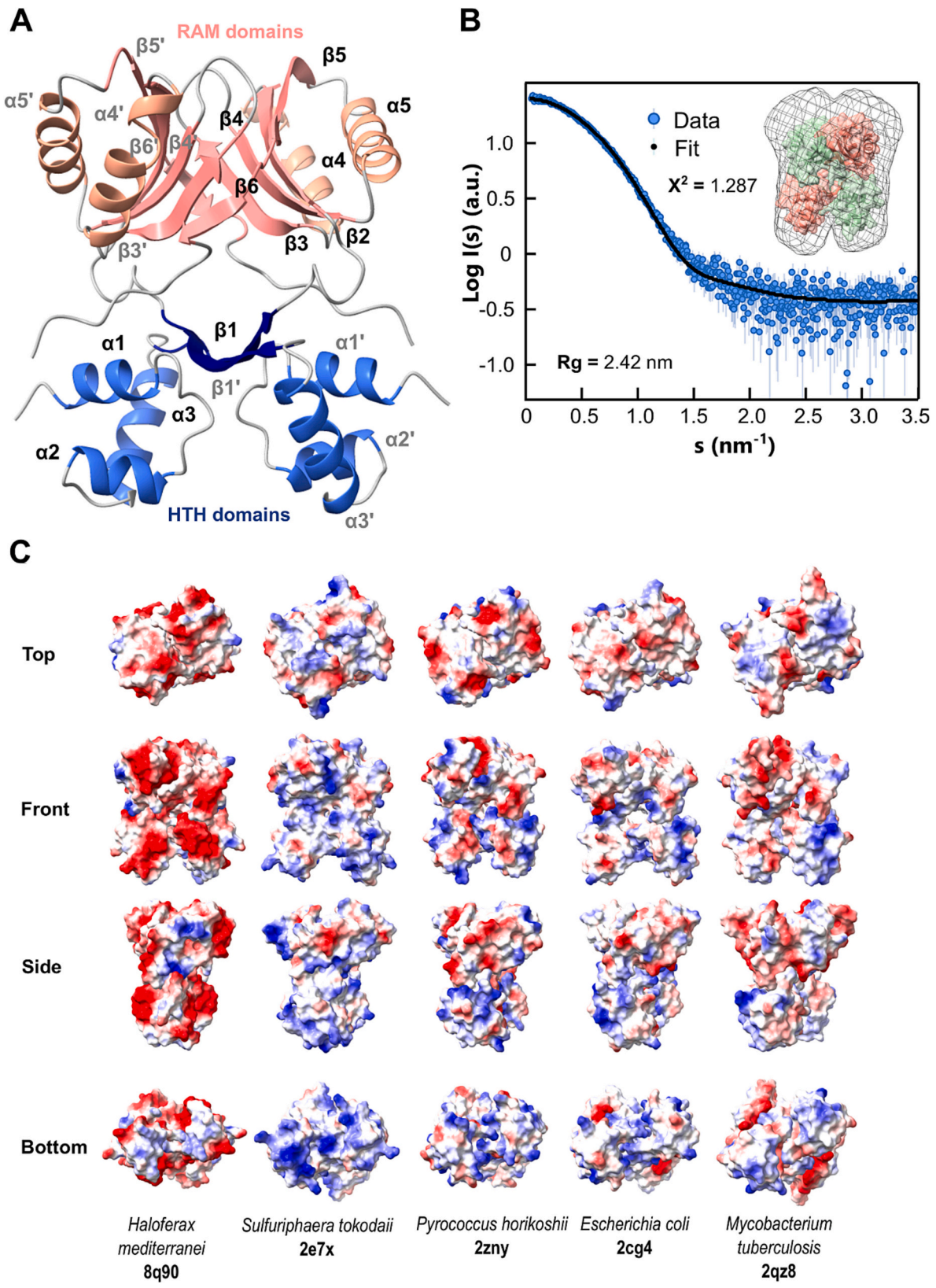

Fig. 4. Structural studies of the Lrp transcription factor. **A.** Homodimeric structure of the Lrp protein from *Hfx. mediterranei*. The blue colour represents the HTH domains, and the pink colour represents the RAM domains. **B.** Lrp scattering curve obtained by SAXS compared with the calculated from the crystal structure using Crysol and surface envelop calculated by Dammin from the scattering curve of Lrp and overlapped with the homodimeric structure. **C.** Surface comparison of Lrp proteins from other species from Bacteria [29] and Archaea [53] domains.

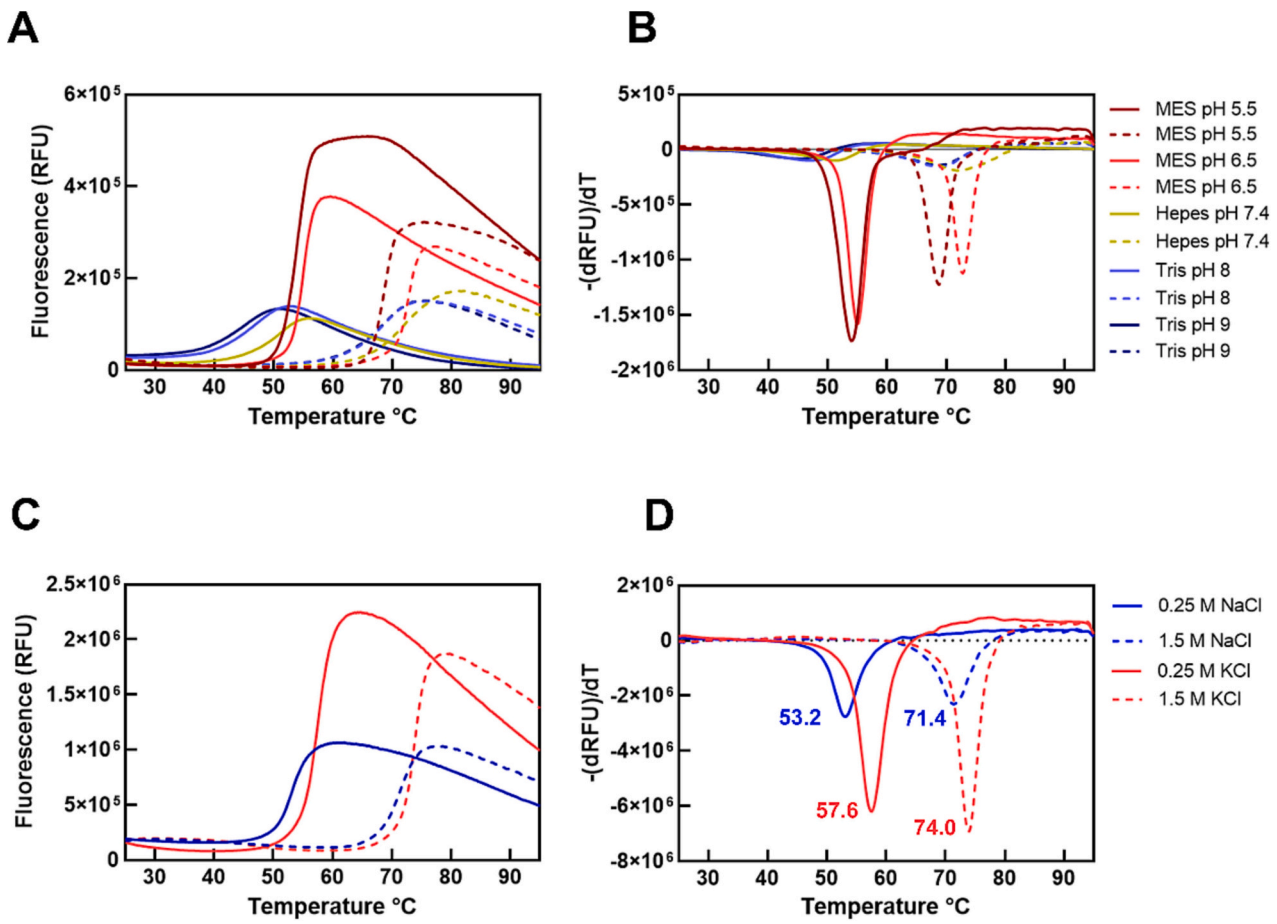

Fig. 5. Thermal shift by DSF to study the effect of pH and low and high salt in the stability of the Lrp transcription factor. Melting curves (**A, C**) and first derivate (**B, D**) from the buffer and salt stability studies (in 50 mM MES pH 6.5).

dimeric winged-helix-turn-helix structure [60]. Halophilic Lrp forms a homodimer as a basic unit, which SAXS has confirmed. Three antiparallel intermolecular β-sheets hold this structure together. The fraction of the solvent-accessible surface of halophilic Lrp is polar, as estimated from our structure, is the highest for any known Lrp protein studied (Fig. 4C), in comparison with Lrp proteins from mesophilic bacteria [29,61] and thermophilic archaea [52,53]. A large polar exposed surface and a low pI (Table S6) should favour protein solubility [62] in a highly saline environment, such as the cytoplasm of *Hfx. mediterranei.* This characteristic is vital for haloadaptation [63–65] as it occurs in other halophilic proteins like glucose dehydrogenase [66] and hmGlnK1, hmGlnK2 [67], preventing it from being salted out.

Nowadays, there is only one structure available of an Lrp protein bound to DNA from *P. horikoshii* (2e1c) [36]. The comparison of the DNA bound and unbound forms from *P. horikoshii* structures (Fig. 6A) suggests that the DNA binding domain suffers a small conformational change that involve the α2 – α3 helices and provokes a displacement of the domains to a modest open state allowing to accommodate the DNA (Fig. 6, represented by black arrows).

The Lrp structure from *Hfx. mediterranei* shows similar level of compactness than the non-bound form (2zny) [53] from *P. horikoshii* (Fig. 6B) giving the idea that small conformational changes might also occur in this Lrp protein, as observed in the DSF experiments when DNA bounds in absence of L-Gln (Fig. S4). Although both Lrp proteins (*P. horikoshii* and *Hfx. mediterranei*) are structurally very similar, their sequences differ considerably by almost 50 % in the full protein and around 40 % in the HTH domain. The residues involved in DNA interaction according to *P. horikoshii* structure [36] are almost semi-conserved (Fig. 6C and D). The structure of *P. horikoshii* Lrp has been shown that the amino acids Ala34-Glu35-Ser36-Thr37 form a loop between helices α2 and α3, and are positioned in the DNA major groove, allowing chemical contacts between amino acids and DNA bases. In the halophilic Lrp, that loop is semi-conserved, Ser32-Val33-Thr34-Thr35 (Fig. 6C) and it might form similar chemical contacts by hydrogen bonds and hydrophobic interactions with DNA bases as occurs in *P. horikoshii*. In addition, in *Hfx, mediterranei* Ser37 and His39 replace His39 and Arg41 from *P. horikoshii.* Even though the DNA interaction region present similar properties (Fig. 6C and D), these small differences in residues might be crucial for the recognition of specific DNA sequences. Arg25 is conserved in *Hfx. mediterranei* (Arg23) but the side chain orientation is affected by the DNA binding.

Structural studies of the Lrp protein from *S. tokadaii* [52] in the presence of L-Gln, shows an extra interactional site at the HTH domain, which it is not required for the oligomerization of the protein. This interaction is mediated by Ser32 in *S. tokadaii*, which is replaced by Thr34 in *Hfx. mediterranei* allowing the same type of interaction to occur. This interaction might be involved in the DNA binding regulation by interfering physically with the DNA binding through that region.

The availability of the structural information of Lrp could help to understand further how Lrp activates the expression of GS and NasA under nitrogen-limiting conditions while repressing their expression in the presence of ammonium. A high concentration of L-Gln inside the cell, a sign of good nitrogen supply, can imply the binding of L-Gln to Lrp transcription factor, avoiding its binding to the promoters of *nasABC* and *glnA* and repressing the expression of these genes. Meanwhile, a low concentration of L-Gln (nitrogen deficit) might induce the activation of the expression of these genes by binding the Lrp transcription factor to the promoters.

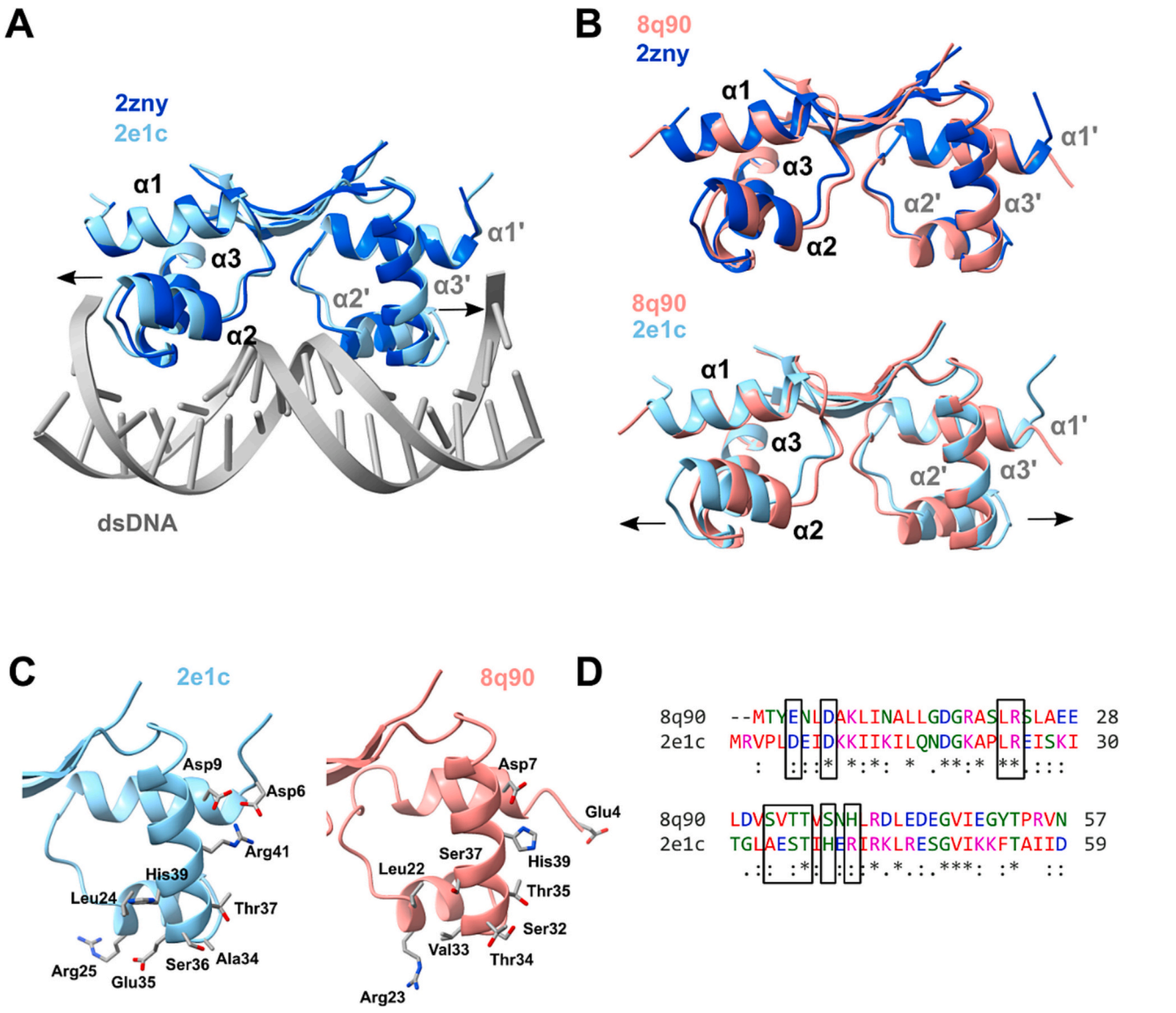

Fig. 6. A. Structure comparison of the Lrp protein from of *P. horikoshii* with (2e1c; cyan) and without (2zny; blue) DNA bound (dsDNA; grey). **B**. Structure comparison of the Lrp protein from *Hfx. mediterranei* (8q90; pink) with *P. horikoshii* bound (2e1c; cyan) and non-bound (2zny; blue) to DNA. The black arrows represents the displacement of the structures. **C**. Representation of the residues involved in DNA binding of *P. horikoshii* (2e1c; cyan) and their respective residues in *Hfx. mediterranei* (8q90; pink). **D**.omprehensive Python-based system for macromolecular structure solution Sequence alignment of the HTH domain of *P. horikoshii* (2e1c) and *Hfx. mediterranei* (8q90) using clustal Omega [68]. The black squares represent the residues from *P. horikoshii* involved in DNA binding.

5. Conclusion

Remarkably, this study constitutes the first direct evidence of a transcriptional regulator's involvement in the nitrogen assimilative pathway in *Hfx. mediterranei*. Our results unequivocally confirm the role played by the Lrp transcriptional regulator in regulating two crucial genes in the nitrogen cycle of *Hfx. mediterranei, glnA* and *nasABC,* apart from its own regulation. These findings shed light on this extremophilic organism's intricate regulatory networks governing nitrogen metabolism. Furthermore, L-Gln acts as a ligand in the Lrp, as demonstrated by EMSA studies, DSF experiments and the retardation in size exclusion chromatography. Depending on its presence or absence, the quaternary structure of Lrp changes from an octamer to a dimer. Other ligands may be involved in the molecular mechanism of this transcriptional regulator. Although the sequence alignment between Lrp proteins from different species shows a low similarity (Fig. S6), the tridimensional structure for these proteins remains highly conserved, except for the highly acidic surface of this halophilic protein, that plays a vital role in adapting halophilic environments.

CRediT authorship contribution statement

Laura Matarredona: Writing – review & editing, Writing – original draft, Methodology, Investigation, Formal analysis, Conceptualization. **María-José García-Bonete:** Writing – review & editing, Writing – original draft, Methodology, Investigation, Formal analysis, Conceptualization. **Jorge Guío:** Writing – review & editing, Methodology. **Mónica Camacho:** Writing – review & editing, Resources, Investigation. **María F. Fillat:** Writing – review & editing, Methodology. **Julia Esclapez:** Writing – review & editing, Supervision, Formal analysis, Conceptualization. **María-José Bonete:** Writing – review & editing, Writing – original draft, Validation, Methodology, Investigation, Conceptualization, Project administration, Funding acquisition.

Declaration of competing interest

The authors declare no conflicts of interest.

Data availability statement

The structural data have been deposited to the Protein Data Bank with accession code 8Q90, and the diffraction images to the Integrated Resource for Reproducibility in Macromolecular Crystallography (IRRMC ID: TBA).

SAXS data has been deposited to the Small Angle Scattering Biological Data Bank with the accession code SASDT82.

Acknowledgments

We thank the beamline scientists at Biomax beamline at MAXIV synchrotron in Lund, Sweden and the beamline scientists at BM29 beamline at ESRF synchrotron in Grenoble, France, for their support and make possible the structural data collection. We would also like to thank the Dept. of Chemistry and Molecular Biology and the Mucin Biology Groups for allowing us to use the crystallography equipment and facilities, especially Dr. Weixiao Y Wahlgren, for her support in this work. We also would like to acknowledge the "Unidad de Genómica y Proteómica de los Servicios Técnicos de Investigación de la Universidad de Alicante" for the accessibility to the real-time PCR machine for the DSF experiments.

Funding for this research was provided by the Ministry of Economy and Competitiveness and FEDER (BIO2013-42921-P); "Programa Propio para el Fomento de la I+D+i del Vicerrectorado de Investigación y Transferencia de Conocimiento" of the University of Alicante (Spain) (GRE20-02-C; VIGROB-016).

Appendix A. Supplementary data

Supplementary data to this article can be found online at https://doi.org/10.1016/j.ijbiomac.2024.129541.

References

[1] F. Rodriguez-Valera, G. Juez, D.J. Kushner, *Halobacterium mediterranei* spec, nov., a new carbohydrate-utilizing extreme halophile, Syst. Appl. Microbiol. 4 (3) (1983) 369–381, https://doi.org/10.1016/S0723-2020(83)80021-6.

[2] M.F. Roberts, Organic compatible solutes of halotolerant and halophilic microorganisms, Saline Syst. 1 (2005) 5, https://doi.org/10.1186/1746-1448-1-5.

[3] M.J. Bonete, R.M. Martínez-Espinosa, C. Pire, B. Zafrilla, D.J. Richardson, Nitrogen metabolism in haloarchaea, Saline Syst. 4 (2008) 9, https://doi.org/10.1186/1746-1448-4-9.

[4] L. Pedro-Roig, C. Lange, M.J. Bonete, J. Soppa, J. Maupin-Furlow, Nitrogen regulation of protein-protein interactions and transcript levels of GlnK PII regulator and AmtB ammonium transporter homologs in Archaea, MicrobiologyOpen 2 (5) (2013) 826–840, https://doi.org/10.1002/mbo3.120.

[5] J. Esclapez, G. Bravo-Barrales, V. Bautista, C. Pire, M. Camacho, M.J. Bonete, Effects of nitrogen sources on the nitrate assimilation in *Haloferax mediterranei*: growth kinetics and transcriptomic analysis, FEMS Microbiol. Lett. 350 (2) (2014) 168–174, https://doi.org/10.1111/1574-6968.12325.

[6] F. Pérez-Pomares, V. Bautista, J. Ferrer, C. Pire, F.C. Marhuenda-Egea, M.J. Bonete, α-Amylase activity from the halophilic archaeon *Haloferax mediterranei*, Extremophiles 7 (4) (2003) 299–306, https://doi.org/10.1007/s00792-003-0327-6.

[7] C. Nájera-Fernández, B. Zafrilla, M.J. Bonete, R.M. Martínez-Espinosa, Role of the denitrifying Haloarchaea in the treatment of nitrite-brines, Int. Microbiol. 15 (3) (2012) 111–119, https://doi.org/10.2436/20.1501.01.164.

[8] J. Torregrosa-Crespo, R.M. Martínez-Espinosa, J. Esclapez, V. Bautista, C. Pire, M. Camacho, D.J. Richardson, M.J. Bonete, Anaerobic metabolism in *Haloferax* genus: denitrification as case of study, Adv. Microb. Physiol. 68 (2016) 41–85, https://doi.org/10.1016/bs.ampbs.2016.02.001.

[9] R.M. Martínez-Espinosa, F.C. Marhuenda-Egea, M.J. Bonete, Assimilatory nitrate reductase from the haloarchaeon *Haloferax mediterranei*: purification and characterisation, FEMS Microbiol. Lett. 204 (2) (2001) 381–385, https://doi.org/10.1016/s0378-1097(01)00431-1.

[10] R.M. Martínez-Espinosa, F.C. Marhuenda-Egea, M.J. Bonete, Purification and characterisation of a possible assimilatory nitrite reductase from the halophile archaeon *Haloferax mediterranei*, FEMS Microbiol. Lett. 196 (2) (2001) 113–118, https://doi.org/10.1111/j.1574-6968.2001.tb10550.x.

[11] V. Rodríguez-Herrero, G. Payá, V. Bautista, A. Vegara, M. Cortés-Molina, M. Camacho, J. Esclapez, M.J. Bonete, Essentiality of the *glnA* gene in *Haloferax mediterranei:* gene conversion and transcriptional analysis, Extremophiles 24 (3) (2020) 433–446, https://doi.org/10.1007/s00792-020-01169-x.

[12] R.M. Martínez-Espinosa, J. Esclapez, V. Bautista, M.J. Bonete, An octameric prokaryotic glutamine synthetase from the haloarchaeon *Haloferax mediterranei*, FEMS Microbiol. Lett. 264 (1) (2006) 110–116, https://doi.org/10.1111/j.1574-6968.2006.00434.x.

[13] J. Ferrer, F. Pérez-Pomares, M.J. Bonete, NADP-glutamate dehydrogenase from the halophilic archaeon *Haloferax mediterranei*: enzyme purification, N-terminal sequence and stability, FEMS Microbiol. Lett. 141 (1) (1996) 59–63, https://doi.org/10.1111/j.1574-6968.1996.tb08363.x.

[14] S. Díaz, F. Pérez-Pomares, C. Pire, J. Ferrer, M.J. Bonete, Gene cloning, heterologous overexpression and optimized refolding of the NAD-glutamate dehydrogenase from *Haloferax mediterranei*, Extremophiles 10 (2) (2006) 105–115, https://doi.org/10.1007/s00792-005-0478-8.

[15] J. Esclapez, C. Pire, M. Camacho, V. Bautista, R.M. Martínez-Espinosa, B. Zafrilla, A. Vegara, L.A. Alcaraz, M.J. Bonete, Transcriptional profiles of *Haloferax mediterranei* based on nitrogen availability, J. Biotechnol. 193 (2015) 100–107, https://doi.org/10.1016/j.jbiotec.2014.11.018.

[16] R.M. Martínez-Espinosa, B. Lledó, F.C. Marhuenda-Egea, S. Díaz, M.J. Bonete, NO_3^-/NO_2^- assimilation in halophilic archaea: physiological analysis, *nasA* and *nasD* expressions, Extremophiles 13 (5) (2009) 785–792, https://doi.org/10.1007/s00792-009-0266-y.

[17] L. Pedro-Roig, M. Camacho, M.J. Bonete, Regulation of ammonium assimilation in *Haloferax mediterranei*: interaction between glutamine synthetase and two GlnK proteins, Biochim. Biophys. Acta 1834 (1) (2013) 16–23, https://doi.org/10.1016/j.bbapap.2012.10.006.

[18] R. Schwaiger, C. Schwarz, K. Furtwängler, V. Tarasov, A. Wende, D. Oesterhelt, Transcriptional control by two leucine-responsive regulatory proteins in *Halobacterium salinarum* R1, BMC Mol. Biol. 11 (2010) 40, https://doi.org/10.1186/1471-2199-11-40.

[19] L. Matarredona, M. Camacho, M.J. García-Bonete, B. Esquerra, B. Zafrilla, J. Esclapez, M.J. Bonete, Analysis of *Haloferax mediterranei* Lrp transcriptional regulator, Genes (Basel) 12 (6) (2021) 802, https://doi.org/10.3390/genes12060802.

[20] L. Lemmens, H.R. Maklad, I. Bervoets, E. Peeters, Transcription regulators in arch aea: homologies and differences with bacterial regulators, J. Mol. Biol. 431 (20) (2019) 4132–4146, https://doi.org/10.1016/j.jmb.2019.05.045.

[21] E. Pérez-Rueda, S.C. Janga, Identification and genomic analysis of transcription factors in archaeal genomes exemplifies their functional architecture and evolutionary origin, Mol. Biol. Evol. 27 (6) (2010) 1449–1459, https://doi.org/10.1093/molbev/msq033.

[22] A.B. Brinkman, T.J.G. Ettema, V.M. de Vos WM, J. van der Oost, The Lrp family of transcriptional regulators, Mol. Microbiol. 48 (2) (2003) 287–294, https://doi.org/10.1046/j.1365-2958.2003.03442.x.

[23] E. Peeters, D. Charlier, The Lrp family of transcription regulators in archaea, Archaea 2010 (2010), https://doi.org/10.1155/2010/750457. Article 750457.

[24] J.M. Calvo, R.G. Matthews, The leucine-responsive regulatory protein, a global regulator of metabolism in *Escherichia coli*, Microbiol. Rev. 58 (3) (1994) 466–490, https://doi.org/10.1128/mr.58.3.466-490.1994.

[25] A.B. Brinkman, S.D. Bell, R.J. Lebbinkt, V.M. de Vos, J. van der Oost, The *Sulfolobus solfataricus* Lrp-like protein LysM regulates lysine biosynthesis in response to lysine availability, J. Biol. Chem. 277 (33) (2002) 29537–29549, https://doi.org/10.1074/jbc.M203528200.

[26] T. Kawashima, H. Aramaki, T. Oyamada, K. Makino, M. Yamada, H. Okamura, K. Yokoyama, S.A. Ishijima, M. Suzuki, Transcription regulation by feast/famine regulatory proteins, FFRPs, in Archaea and Eubacteria, Biol. Pharm. Bull. 31 (2) (2008) 173–186, https://doi.org/10.1248/bpb.31.173.

[27] A. Vassart, M. Van Wolferen, A. Orell, Y. Hong, E. Peeters, S.-V. Albers, D. Charlier, Sa-Lrp from *Sulfolobus acidocaldarius* is a versatile, glutamine-responsive, and architectural transcriptional regulator, MicrobiologyOpen 2 (1) (2013) 75–93, https://doi.org/10.1002/mbo3.58.

[28] S. Chen, J.M. Calvo, Leucine-induced dissociation of *Escherichia coli* Lrp Hexadecamers to octamers, J. Mol. Biol. 318 (4) (2002) 1031–1042, https://doi.org/10.1016/S0022-2836(02)00187-0.

[29] P. Thaw, S.E. Sedelnikova, T. Muranova, S. Wiese, S. Ayora, J.C. Alonso, A. B. Brinkman, J. Akerboom, J. van der Oost, J.B. Rafferty, Structural insight into gene transcriptional regulation and effector binding by the Lrp/AsnC family, Nucleic Acids Res. 34 (5) (2006) 1439–1449, https://doi.org/10.1093/nar/gkl009.

[30] J. Ren, S. Sainsbury, S.E. Combs, R.G. Capper, P.W. Jordan, N.S. Berrow, D. K. Stammers, N.J. Saunders, R.J. Owens, The structure and transcriptional analysis of a global regulator from *Neisseria meningitidis*, J. Biol. Chem. 282 (19) (2007) 14655–14664, https://doi.org/10.1074/jbc.M701082200.

[31] L. Matarredona, M. Camacho, V. Bautista, M.J. Bonete, J. Esclapez, Lrp as a potential transcriptional regulator involved in stress response in *Haloferax mediterranei*, Biochimie 209 (2023) 61–72, https://doi.org/10.1016/j.biochi.2023.01.012.

[32] S. Pastor-Soler, M. Camacho, V. Bautista, M.J. Bonete, J. Esclapez, Towards the elucidation of assimilative *nasABC* operon transcriptional regulation in *Haloferax mediterranei*, Genes (Basel) 12 (5) (2021) 619, https://doi.org/10.3390/genes12050619.

[33] V. Rodríguez-Herrero, A. Peris, M. Camacho, V. Bautista, J. Esclapez, M.J. Bonete, Novel glutamate-putrescine ligase activity in *Haloferax mediterranei*: a new function for *glnA-2* gene, Biomolecules 11 (8) (2021) 1156, https://doi.org/10.3390/biom11081156.

[34] J. Guío, C. Sarasa-Buisan, A. Velázquez-Campoy, M.T. Bes, M.F. Fillat, M. L. Peleato, E. Sevilla, 2-Oxoglutarate modulates the affinity of FurA for the *ntcA* promoter in *Anabaena* sp. PCC 7120, FEBS Lett. 594 (2) (2020) 278–289, https://doi.org/10.1002/1873-3468.13610.
[35] W. Kabsch, XDS. Acta Cryst. D66 (Pt 2) (2010) 125–132, https://doi.org/10.1107/S0907444909047337.
[36] K. Yokoyama, S.A. Ishijima, H. Koike, C. Kurihara, A. Shimowasa, M. Kabasawa, T. Kawashima, M. Suzuki, Feast/famine regulation by transcription factor FL11 for the survival of the Hyperthermophilic archaeon *Pyrococcus* OT3, Structure 15 (12) (2007) 1542–1554, https://doi.org/10.1016/j.str.2007.10.015.
[37] A.J. McCoy, R.W. Grosse-Kunstleve, P.D. Adams, M.D. Winn, L.C. Storoni, R. J. Read, Phaser crystallographic software, J. Appl. Crystallogr. 40 (Pt 4) (2007) 658–674, https://doi.org/10.1107/S0021889807021206.
[38] P.D. Adams, P.V. Afonine, G. Bunkóczi, V.B. Chen, I.W. Davis, N. Echols, J. J. Headd, L-W. Hung, G.J. Kapral, R.W. Grosse-Kunstleve, A.J. McCoy, N. W. Moriarty, R. Oeffner, R.J. Read, D.C. Richardson, J.S. Richardson, T. C. Terwilliger, P.H. Zwart, *PHENIX*: a comprehensive Python-based system for macromolecular structure solution, Acta Cryst. D 66 (Pt 2) (2010) 213–221, https://doi.org/10.1107/S0907444909052925.
[39] D. Liebschner, P.V. Afonine, M.L. Baker, G. Bunkoczi, V.B. Chen, T.I. Croll, B. Hintze, L.W. Hung, S. Jain, A.J. McCoy, N.W. Moriarty, R.D. Oeffner, B.K. Poon, M.G. Prisant, R.J. Read, J.S. Richardson, D.C. Richardson, M.D. Sammito, O. V. Sobolev, D.H. Stockwell, T.C. Terwilliger, A.G. Urzhumtsev, L.L. Videau, C. J. Williams, P.D. Adams, Macromolecular structure determination using X-rays, neutrons and electrons: recent developments in *Phenix*, Acta Crystallogr. D75 (Pt 10) (2019) 861–877, https://doi.org/10.1107/S2059798319011471.
[40] T.C. Terwilliger, R.W. Grosse-Kunstleve, P.V. Afonine, N.W. Moriarty, P.H. Zwart, L.W. Hung, R.J. Read, P.D. Adams, Iterative model building, structure refinement and density modification with the *PHENIX AutoBuild* wizard, Acta Crystallogr. D64 (Pt 1) (2008) 61–69, https://doi.org/10.1107/S090744490705024X.
[41] P. Emsley, B. Lohkamp, W.G. Scott, K. Cowtan, Features and development of *coot*, Acta Crystallogr. D66 (Pt 4) (2010) 486–501, https://doi.org/10.1107/S0907444910007493.
[42] P.V. Afonine, R.W. Grosse-Kunstleve, N. Echols, J.J. Headd, N.W. Moriarty, M. Mustyakimov, T.C. Terwilliger, A. Urzhumtsev, P.H. Zwart, P.D. Adams, Towards automated crystallographic structure refinement with *phenix.refine*, Acta Crystallogr. D68 (Pt 4) (2012) 352–367, https://doi.org/10.1107/S0907444912001308.
[43] P.V. Konarev, V.V. Volkov, A.V. Sokolova, M.H.J. Koch, D.I. Svergun, *PRIMUS*: a windows PC-based system for small-angle scattering data analysis, J. Appl. Crystallogr. 36 (2003) 1277–1282, https://doi.org/10.1107/S0021889803012779.
[44] K. Manalastas-Cantos, P.V. Konarev, N.R. Hajizadeh, A.G. Kikhney, M. V. Petoukhov, D.S. Molodenskiy, A. Panjkovich, H.D.T. Mertens, A. Gruzinov, C. Borges, C.M. Jeffries, D.I. Svergun, D. Franke, *ATSAS 3.0*: expanded functionality and new tools for small-angle scattering data analysis, J. Appl. Crystallogr. 54 (2021) 343–355, https://doi.org/10.1107/S1600576720013412.
[45] D.I. Svergun, Determination of the regularization parameter in indirect-transform methods using perceptual criteria, J. Appl. Crystallogr. 25 (1992) 495–503, https://doi.org/10.1107/S0021889892001663.
[46] N.R. Hajizadeh, D. Franke, C.M. Jeffries, D.I. Svergun, Consensus Bayesian assessment of protein molecular mass from solution X-ray scattering data, Sci. Rep. 8 (1) (2018) 7204, https://doi.org/10.1038/s41598-018-25355-2.
[47] D.I. Svergun, Restoring low resolution structure of biological macromolecules from solution scattering using simulated annealing, Biophys. J. 76 (6) (1999) 2879–2886, https://doi.org/10.1016/S0006-3495(99)77443-6.
[48] D. Svergun, C. Barberato, M.H.J. Koch, *CRYSOL* – a program to evaluate X-ray solution scattering of biological macromolecules from atomic coordinates, J. Appl. Crystallogr. 28 (6) (1995) 768–773, https://doi.org/10.1107/S0021889895007047.
[49] E.F. Pettersen, T.D. Goddard, C.C. Huang, E.C. Meng, G.S. Couch, T.I. Croll, J. H. Morris, T.E. Ferrin, U.C.S.F. ChimeraX, Structure visualization for researchers, educators, and developers, Protein Sci. 30 (1) (2021) 70–82, https://doi.org/10.1002/pro.3943.
[50] J. Chen, R. Mitra, H. Xiang, J. Han, Deletion of the *pps*-like gene activates the cryptic *phaC* genes in *Haloferax mediterranei*, Appl. Microbiol. Biotechnol. 104 (22) (2020) 9759–9771, https://doi.org/10.1007/s00253-020-10898-0.
[51] P.D. Leitner, I. Vietor, L.A. Huber, T. Valovka, Fluorescent thermal shift-based method for detection of NF-κB binding to double-stranded DNA, Sci. Rep. 11 (1) (2021), https://doi.org/10.1038/s41598-021-81743-1. Article 2331.
[52] T. Kumarevel, N. Nakano, K. Ponnuraj, S.C.B. Gopinath, K. Sakamoto, A. Shinkai, P.K.R. Kumar, S. Yokoyama, Crystal structure of glutamine receptor protein from *Sulfolobus tokodaii* strain 7 in complex with its effector L -glutamine: implications of effector binding in molecular association and DNA binding, Nucleic Acids Res. 36 (14) (2008) 4808–4820, https://doi.org/10.1093/nar/gkn456.
[53] M. Yamada, S.A. Ishijima, M. Suzuki, Interactions between the archaeal transcription repressor FL11 and its coregulators lysine and arginine, Proteins 74 (2) (2009) 520–525, https://doi.org/10.1002/prot.22269.
[54] D.J. Kushner, Molecular adaptation of enzymes, metabolic systems and transport systems in halophilic bacteria, FEMS Microbiol. Rev. 2 (1–2) (1986) 121–127, https://doi.org/10.1111/j.1574-6968.1986.tb01852.x.
[55] M.L. Camacho, R.A. Brown, M.J. Bonete, M.J. Danson, D.W. Hough, Isocitrate dehydrogenases from *Haloferax volcanii* and *Sulfolobus solfataricus*: enzyme purification, characterisation and N-terminal sequence, FEMS Microbiol. Lett. 134 (1) (1995) 85–90, https://doi.org/10.1111/j.1574-6968.1995.tb07919.x.
[56] M.J. Bonete, C. Pire, F.I. Llorca, M.L. Camacho, Glucose dehydrogenase from the halophilic archaeon *Haloferax mediterranei*: enzyme purification, characterisation and N-terminal sequence, FEBS Lett. 383 (3) (1996) 227–229, https://doi.org/10.1016/0014-5793(96)00235-9.
[57] J.A. Serrano, M. Camacho, M.J. Bonete, Operation of glyoxylate cycle in halophilic archaea: presence of malate synthase and isocitrate lyase in *Haloferax volcanii*, FEBS Lett. 434 (1–2) (1998) 13–16, https://doi.org/10.1016/s0014-5793(98)00911-9.
[58] D. Madern, M. Camacho, A. Rodríguez-Arnedo, M.J. Bonete, G. Zaccai, Salt-dependent studies of NADP-dependent isocitrate dehydrogenase from the halophilic archaeon *Haloferax volcanii*, Extremophiles 8 (5) (2004) 377–384, https://doi.org/10.1007/s00792-004-0398-z.
[59] H. Okamura, K. Yokoyama, H. Koike, M. Yamada, A. Shimowasa, M. Kabasawa, T. Kawashima, M. Suzuki, A structural code for discriminating between transcription signals revealed by the feast/famine regulatory protein DM1 in complex with ligands, Structure 15 (10) (2007) 1325–1338, https://doi.org/10.1016/j.str.2007.07.018.
[60] N. Kutnowski, F. Shmulevich, G. Davidov, A. Shahar, D. Bar-Zvi, J. Eichler, R. Zarivach, B. Shaanan, Specificity of protein-DNA interactions in hypersaline environment: structural studies on complexes of *Halobacterium salinarum* oxidative stress-dependent protein *hs*RosR, Nucleic Acids Res. 47 (16) (2019) 8860–8873, https://doi.org/10.1093/nar/gkz604.
[61] M.C.M. Reddy, K. Gokulan, W.R. Jacobs Jr., T.R. Ioerger, J.C. Sacchettini, Crystal structure of *mycobacterium tuberculosis* LrpA, a leucine-responsive global regulator associated with starvation response, Protein Sci. 17 (1) (2007) 159–170, https://doi.org/10.1110/ps.073192208.
[62] C. Tanford, Physical Chemistry of Macromolecules, second ed., John Wiley & Sons, New York, 1967.
[63] H. Eisenberg, M. Mevarech, G. Zaccai, Biochemical, structural, and molecular genetic aspects of halophilism, Adv. Protein Chem. 43 (1992) 1–62, https://doi.org/10.1016/s0065-3233(08)60553-7.
[64] S. Paul, S.K. Bag, S. Das, E.T. Harvill, C. Dutta, Molecular signature of hypersaline adaptation: INSIGHTS from genome and proteome composition of halophilic prokaryotes, Genome Biol. 9 (4) (2008), https://doi.org/10.1186/gb-2008-9-4-r70. Article R7.
[65] A. Siglioccolo, A. Paiardini, M. Piscitelli, S. Pascarella, Structural adaptation of extreme halophilic proteins through decrease of conserved hydrophobic contact surface, BMC Struct. Biol. 11 (2011), https://doi.org/10.1186/1472-6807-11-50. Article 50.
[66] K.L. Britton, P.J. Baker, M. Fisher, S. Ruzheinikov, D.J. Gilmour, M.J. Bonete, J. Ferrer, C. Pire, J. Esclapez, D.W. Rice, Analysis of protein solvent interactions in glucose dehydrogenase from the extreme halophile *Haloferax mediterranei*, Proc. Natl. Acad. Sci. U SA 103 (13) (2006) 4846–4851, https://doi.org/10.1073/pnas.0508854103.
[67] C. Palanca, L. Pedro-Roig, J.L. Llácer, M. Camacho, M.J. Bonete, V. Rubio, The structure of a PII signaling protein from a halophilic archaeon reveals novel traits and high-salt adaptations, FEBS J. 281 (15) (2014) 3299–3314, https://doi.org/10.1111/febs.12881.
[68] F. Madeira, M. Pearce, A.R.N. Tivey, P. Basutkar, J. Lee, O. Edbali, N. Madhusoodanan, A. Kolesnikov, R. Lopez, Search and sequence analysis tools services from EMBL-EBI in 2022, Nucleic Acids Res. 50 (W1) (2022) W276–W279, https://doi.org/10.1093/nar/gkac240.